Chapter 3

Dynamic light scattering study of the viscoelastic twist mode in a cholesteric

3.1 Introduction

In liquid crystals, thermal fluctuations of the average direction of the orientation of the molecules (the director) result in strong dielectric tensor fluctuations causing intense scattering of light. Here, dynamic light scattering **(DLS)** experiments reveal relaxation times of the thermally excited modes of director fluctuations. In cholesteric liquid crystals the molecules are locally arranged in planes of uniaxial symmetry (symmetry axis parallel to the director n) which twists gradually giving rise to a helical structure. In such a structure, any arbitrary fluctuation can be resolved into modes with their wavevectors respectively parallel or perpendicular to the twist axis. Further, it can be shown that there are two modes with wavevectors parallel to the twist axis. These will couple strongly to the incident light [1]. The first of these modes, called the *twist mode* has director fluctuations within a plane perpendicular to the twist axis. The second of these modes called the *umbrella* mode has out of plane director fluctuations perpendicular to the twist axis.

In the present chapter, we investigate the twist mode by dynamic light scattering. The twist mode fluctuations give rise to the winding and unwinding of the helical cholesteric structure. We establish, experimentally the dispersion curve for the twist mode in a wavevector regime comparable to the equilibrium cholesteric wave vector

q_0. Du Pre et.al.[2], **[3]** have studied these modes in a lyotropic cholesteric liquid crystal where the wavevector of the cholesteric helix is about two orders of magnitude smaller than that of the incident light. Their experiments were carried out in the frequency domain where they could observe the broadening of the Rayleigh line width corresponding to the two modes. The large difference between wavelength of light and pitch did not allow them to probe the dynamics of the cholesteric structure at length scales comparable to the pitch.

We report a systematic experimental investigation of the twist mode in a thermotropic cholesteric liquid crystal where the wavelength of the incident light is comparable to the cholesteric pitch. This criterion allows us to probe the dynamics of the system at wavevectors that were not accessible to the previous investigators.

3.2 Theory

Followingde Gennes [4] we consider director fluctuations in cholesterics with wavevectors along the twist axis. The twist mode is treated as a thermally induced perturbation about the equilibrium cholesteric structure. Assuming the twist axis to be along the z axis, the director components in the presence of the twist fluctuations can be described by

$$\begin{aligned} n_x &= cos(q_0\, z + u) \\ n_y &= sin(q_0\, z + u) \\ n_z &= 0 \end{aligned} \tag{3.1}$$

Here $q_0 = 2\pi/P$, P is the pitch of the cholesteric, and u is a dimensionless fluctuation amplitude profile. The amplitude u can be Fourier decomposed into components each having a wavevector l. It can be written as,

$$u = \sum_{l=0}^{\infty} u_0^l e^{ilz} \tag{3.2}$$

This type of twist deformation leads to an off-diagonal (xy) component of the dielectric tensor **[4]** given by,

$$\epsilon_{x,y} = \epsilon_a\{n_x^\circ \delta n_y + n_y^\circ \delta n_x\} = \frac{\epsilon_a}{2}\{e^{i2q_\circ z} + e^{-i2q_\circ z}\}u_\circ e^{ilz}$$

Thus, it is associated with the scattering wavevector

$$q = l \pm 2q_\circ$$

For pure twist deformations in the cholesterics, we can write the distortion free energy density as,

$$\begin{aligned} F_d &= K_2((\mathbf{n}\cdot\nabla\times\mathbf{n}) + q_\circ)^2 \\ &= K_2\left(\frac{\partial\theta'}{\partial z} - q_o\right)^2 \end{aligned} \tag{3.3}$$

Here, $\theta'=(q_0 z + \mathrm{u})$ and K_2 is the twist elastic constant.

The Langevin equation for the dyriamical variable θ' is,

$$\gamma_1\frac{\partial\theta'}{\partial t} = -\frac{\delta F_d}{\delta\theta'}$$

Where right hand side is the functional derivative of F_d and γ_1 is the twist viscosity coefficient. Now,

$$\frac{\delta E_d}{\delta\theta'} = -K_2\frac{\partial^2 \theta}{\partial X^2}$$

Hence we get,

$$\gamma_1\frac{\partial\theta'}{\partial t} = K_2\frac{\partial^2\theta'}{\partial z^2} \tag{3.4}$$

Hence,

$$\gamma_1\frac{\partial u(z,t)}{\partial t} = K_2\frac{\partial^2 u(z,t)}{\partial z^2}$$

In the Fourier space $u(z,t)$ can be writteri as a summation of its individual modes ie.,

$$u(z,t) = \sum_l u_\circ^l(t)e^{ilz}$$

The equation of motion of the *lth* mode is given by

$$\gamma_1 \frac{\partial u_o^l(t)}{\partial t} = -K_2 l^2 u_o^l(t) \tag{3.5}$$

Hence, one can obtain an expression for the damping rate 1/71 of the amplitude of the mode with wavevector l

$$\frac{1}{\tau_l} = \frac{K_2 l^2}{\gamma_1} \tag{3.6}$$

Since the optical periodicity in the cholesteric is half the pitch, $2q_o$ is the wavevector corresponding to the optical periodicity sensed by the incident light. Here, $l = q \mp 2q_o$. It can be seen that the relaxation rate of the twist fluctuation goes to zero as the scattering wavevector q approaches the optical wavevector $2q_o$ of the sample. This result can also be understood intuitively by looking upon the equilibrium twist of the cholesteric as a "frozen in" fluctuation having an infinitely long relaxation time. The director fluctuations couple to the incident light via the dielectric tensor components. This fluctuating intensity falling on a detector gives an output in the form of a train of randomly bunched pulses. From this pulse train the intensity autocorrelation function can be obtained. This is related to the electric field autocorrelation function via the Siegret relation already described in chapter *2*

$$g_2(\tau) = 1 + \beta |g_1(\tau)|^2$$

Here β is a coherence factor that depends on experimental conditions like coherence area, average intensity etc. It is a measure of the signal to noise ratio in the experiment. The experimentally obtained dispersion curves are fitted to a polynomial of degree *2* to obtain the pitch and the viscoelastic coefficient. We discuss this in more detail in section 4.

3.3 Experimental

In our experiments the cholesteric sample is illuminated with light of wavelength comparable to its pitch. The cholesteric sample is aligned with its twist axis perpendicular to plane of the cell. For a certain orientation of the cell with respect to

the incident light, a prominent Bragg reflection can be seen in the back scattering arrangement. We have performed our experiments in the vicinity of the Bragg reflection since scattering due to twist fluctuations is very prominent in this direction. The laser used in our experiments was a 488nm Argon ion laser. Since none of the readily available cliolesteric compounds had a pitch comparable to this wavelength, we had to prepare mixtures of compounds with opposite helicities in various proportions so that we got a cholesteric with a desired pitch. In the following section we describe the way we prepared our samples.

3.3.1 Sample preparation

The cholesteric liquid crystal used in our experiment was a three component mixture. We start with cholesteryl chloride (CCL), which is a right handed cliolesteric material. We mix CCL in different proportions with cholesteryl nonanoate (CNN), which is a left handed cholesteric material, till we get a cliolesteric mixture of desired pitch. One can get a rough estimate of the pitch by simply observing the color of the light reflected from an aligned sample. The sample has to be aligned with its twist axis perpendicular to the glass plate, illuminated with white light and viewed against a dark background. Once the pitch is in the required range more accurate estimates can be obtained by selective reflection experiments. Both CCL and CNN are crystalline at room temperature. Although the mixture of CCL and CNN initially seemed be cholesteric at room temperature we found that after a few hours it begins to crystallize. To prevent crystallization we add a third component, cholesteryl oleyl carbonate (COC), which is left handed and a room temperature cholesteric. We found that COC prevented crystallization without affecting the pitch very much. All three compounds were obtained from Aldrich Co. The transition temperatures of the individual components are shown in figure(3.1). The final mixture used in the experiments had the following proportions (by weight percent) of the compounds. CCL-63.86, CCN-26.57 and COC-9.8. The mixture was a room temperature cholesteric.

The sample cells were prepared with clean untreated glass plates. Mylar sheets were

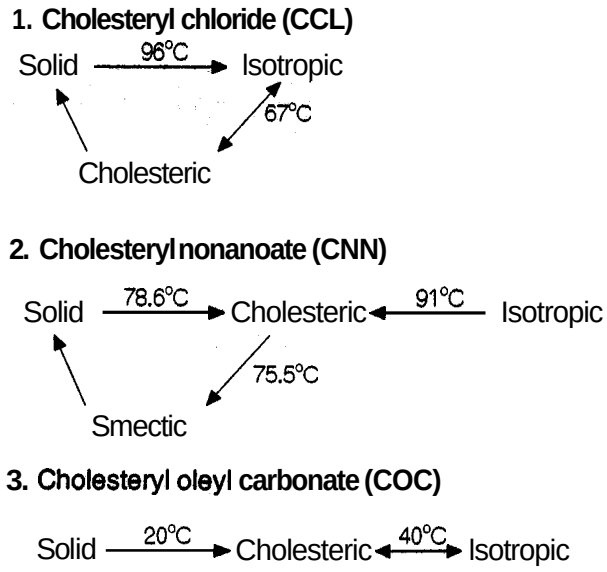

Figure **3.1:** Showing the phase sequence and transition temperatures of the three pure compounds used in the experiments.

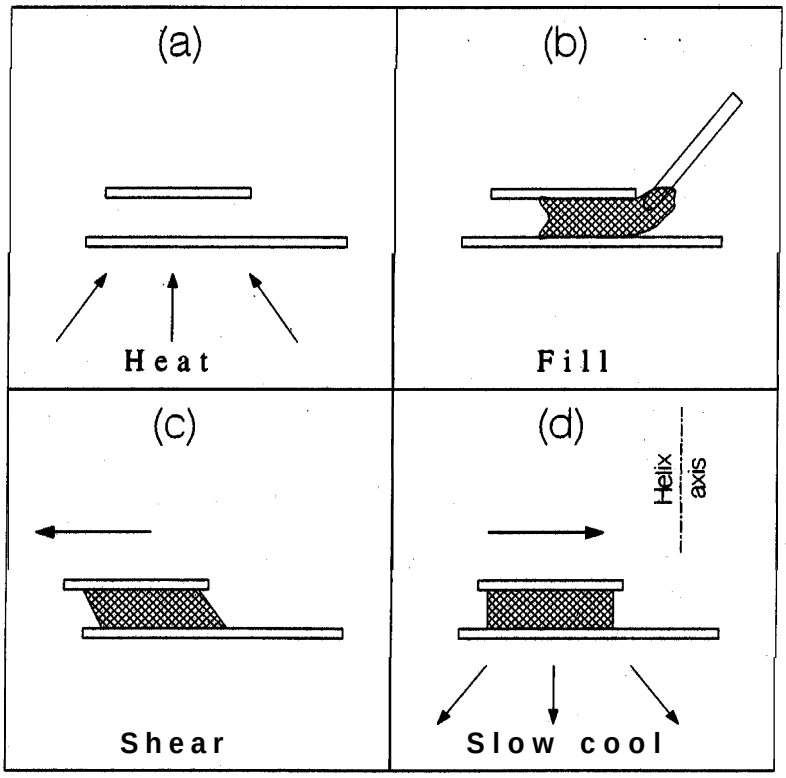

Figure 3.2: The procedure to get cholesteric samples aligned with the twist axis perpendicular to the cell walls.

used as spacers. The glass plates were held together with uncured epoxy glue. The glue was not cured since the plates had to be sheared after filling the cell with the sample. The cell was pre-heated to a temperature above the isotropic temperature of the mixture which entered the cell because of capillarity. As the cell was cooled, the plates were gently sheared with respect to each other. This process induced an alignment of the cholesteric with its twist axis perpendicular to the cell walls. The alignment procedure is schematically depicted in figure(3.2). The cholesteric-isotropic phase transition occurred over small range of temperatures (f1°C) centered around 62.8°C. The transition was observed under a polarizing microscope with the sample cell placed in a hot stage (Mettler FP82HT, f 0.1°C). In the presence of white light, characteristic iridiscent colors were seen indicating that the pitch was comparable to the wavelength of visible light. The cell was checked under a polarizing microscope (Leitz Orthoplan) and uniform texture was observed confirming a good alignment. Between crossed polaroids the cell looked predominantly red. When the analyzer is parallel to the polarizer the color changes to bright green.

The pitch of the sample was determined from the transmission spectrum obtained using a double beam spectrophotometer (Hitachi U-3200). The well defined minimum in the spectrum is the center of the Bragg reflection band (λ_0) which is related to the pitch of the cholesteric by the well known relation [5],

$$\lambda_0 = \bar{\mu} P$$

Here $\bar{\mu}$ is the average refractive index of the medium and P is the pitch of the cholesteric. The cell was then hermetically sealed with an epoxy glue.

3.3.2 Experimental set up and scattering geometry

In light scattering experiments the measured scattering angles and the actual scattering angles can greatly differ due to refraction of the scattered light at the air-sample-cell interface. The refraction can be reduced by surrounding the sample cell in a cylindrical glass container filled with a medium whose refractive index is close

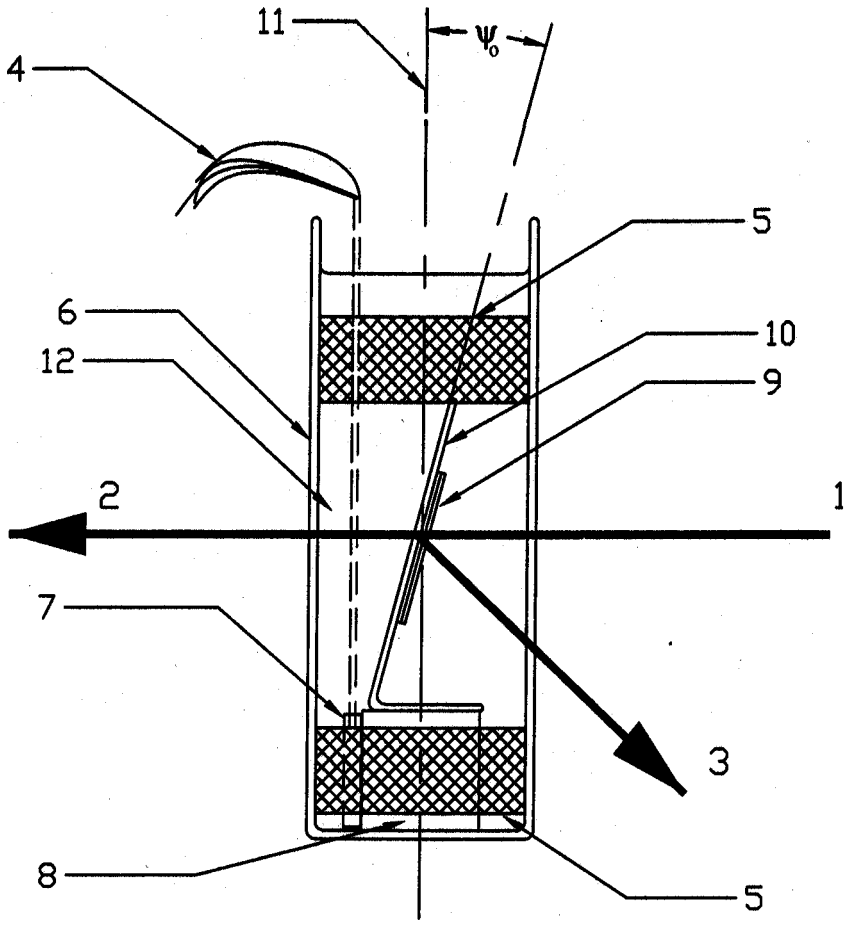

Figure 3.3: A detailed drawing of the refractive index matched sample cell along with the oven. (1) The incident beam. (2) The unscattered beam.(3) The specular reflection from the front of the sample cell. (4) The electrical leads for the heaters and resistance temperature device (RTD). (5) The Kapton strip heaters. (6) The cylindrical glass tube. (7) The liquid immersion type RTD. (8) A copper block. (9) The sample cell containing the cholesteric liquid crystal. (10) The soft wire frame. (11)The goniometer and oven axis. (12)The refractive index matching medium. ψ_o is a small angle through which the sample is tilted to avoid the specularly reflected beam from entering the detector.

to the material of the sample cell, usually glass. Light scattering was performed in a specially designed oven filled with glycerine which acted both as a refractive index matching fluid and a heat transferring medium. The details of the refractive index matched sample oven is shown in figure(3.3).

A proportional integral (PI) temperature control algorithm was implemented on a PC which could maintain sample temperature to an accuracy of $\pm$ 0.1 ^oC. Light from a 488nm Argon ion laser (Spectra Physics, 163), polarized vertically with respect to the scattering plane (which was chosen to be horizontal) was incident on the sample cell

placed inside the oven at the center of the goniometer (Malvern Instruments). The scattered light was detected by a photon counting photomultiplier tube (Electron Tubes Ltd.,9863/KB) housed in an assembly mounted on the goniometer arm. An analyzer placed in front of the photomultiplier tube (PMT) selects the polarization of the detected light. Signals from the PMT were fed to an amplifier-discriminator followed by a digital correlator (Malvern 7200c). The correlator is an 8-bit 256 channel system which facilitated measurements over a wide range of delay times. The digital autocorrelator is interfaced to a PC on which the correlograms are displayed. The photomultiplier tube is mounted on the moving goniometer arm allowing us to obtain correlograms at various angles.The experiments were carried out in the arrangement shown in figurc(3.4).

In the arrangement depicted in figure(3.4), Bragg reflection leads to an intense patch of light for a particular orientation of the sample cell with respect to the incident light. A simple geometric construction shows that when the cell normal exactly bisects the scattering angle, the scattering wavevector lies strictly along the twist axis of the cholesteric. The dispersion curve is obtained by plottixig the relaxation time against the scattering wavevector. A typical dispersion curve obtained in our experiment is shown in figure(3.5).

In our experiments the sample orientation is adjusted so that the scattering wavevector is parallel to the twist axis at every angle. In spite of having an index matched fluid surrounding the sarnple cell, we could still observe a faint specular reflection from the surface of the glass cell. In order to prevent the specular reflection from entering the detector, the sarnple cell is slightly tilted with respect to the scattering plane. The specular reflection now hits the goniometer arm and serves as a useful reference marker during the experiment. A typical raw autocorrelation function obtained in our experiments is shown in figure(3.6). Since the pure twist mode is being detected, the autocorrelatiori can be fitted by a single exponential decay.

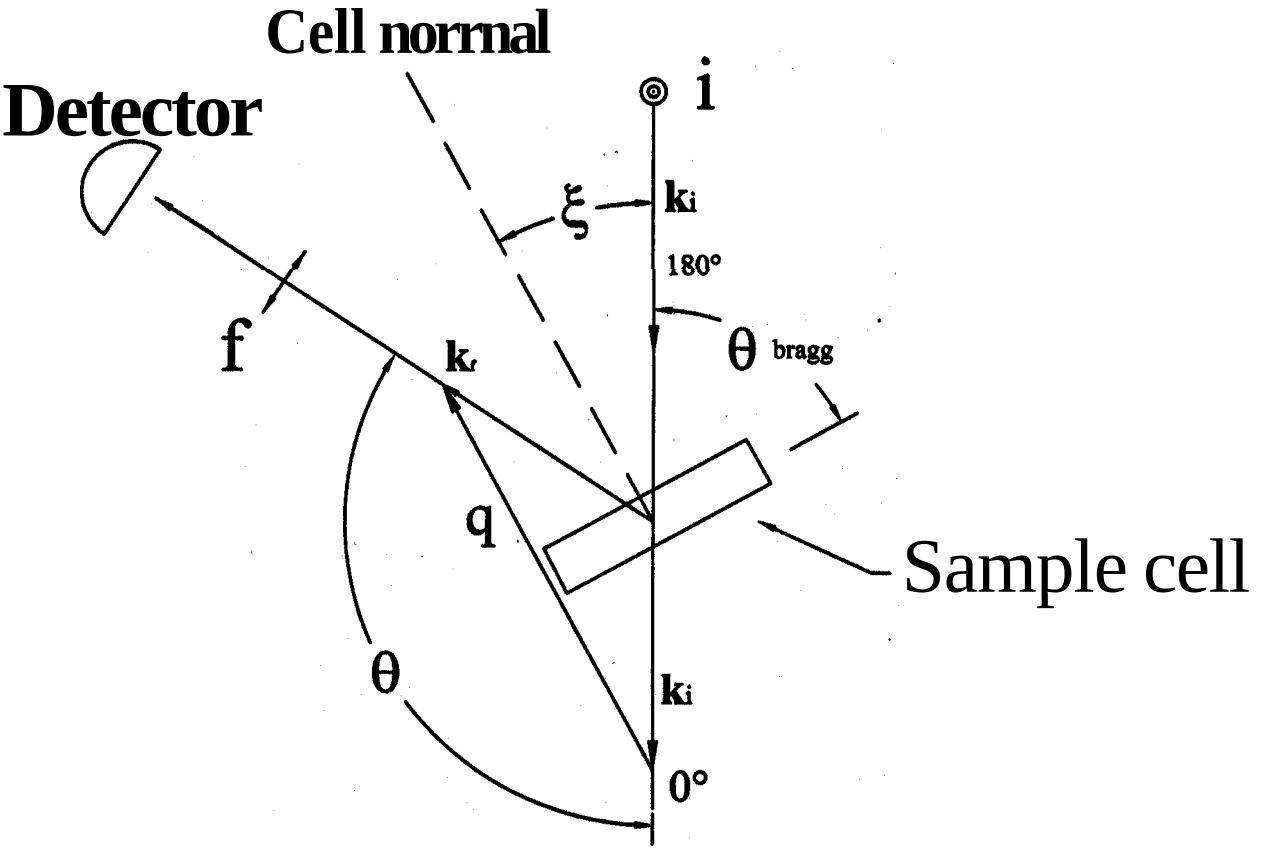

Figure 3.4: The scattering arrangement used in the experiment. Here, the sample is aligned such that the twist axis is parallel to the cell normal. The vectors $\mathbf{k}_i$ and $\mathbf{k}_s$ are the directions of the incident and the scattered wavevectors and q is the scattering wavevector. ξ is the angle made by the cell normal with respect to the incident light and maintained such that q is always parallel to the twist axis. θ is the total scattering angle.

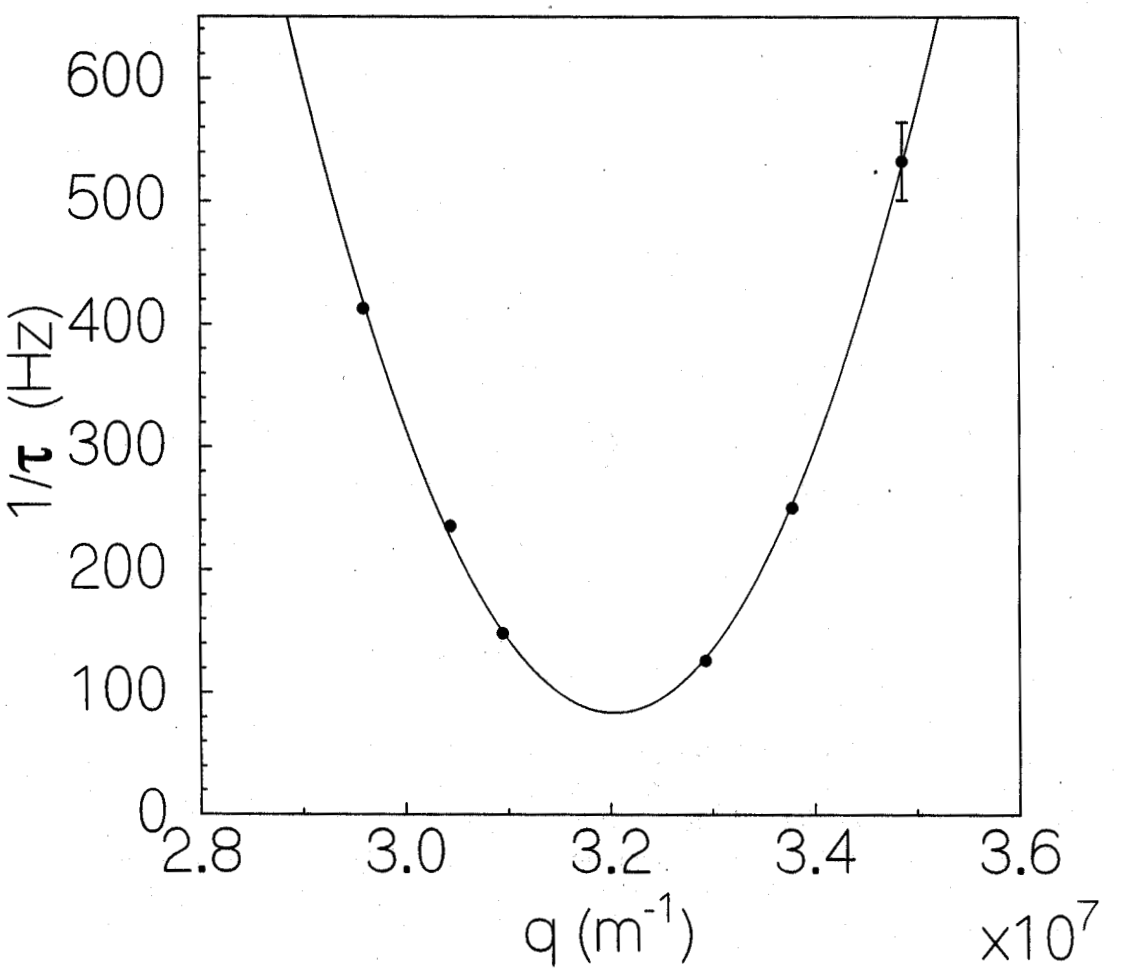

Figure 3.5: Tlie twist mode dispersion curve obtained at 50±0.05 °C. The solid line is a least square fit of a quadratic function to the experimental points. Tlie value of K_2/γ_1 from this data is 5.558 ± 0.007 x $10^{-11} m^2 s^{-1}$.

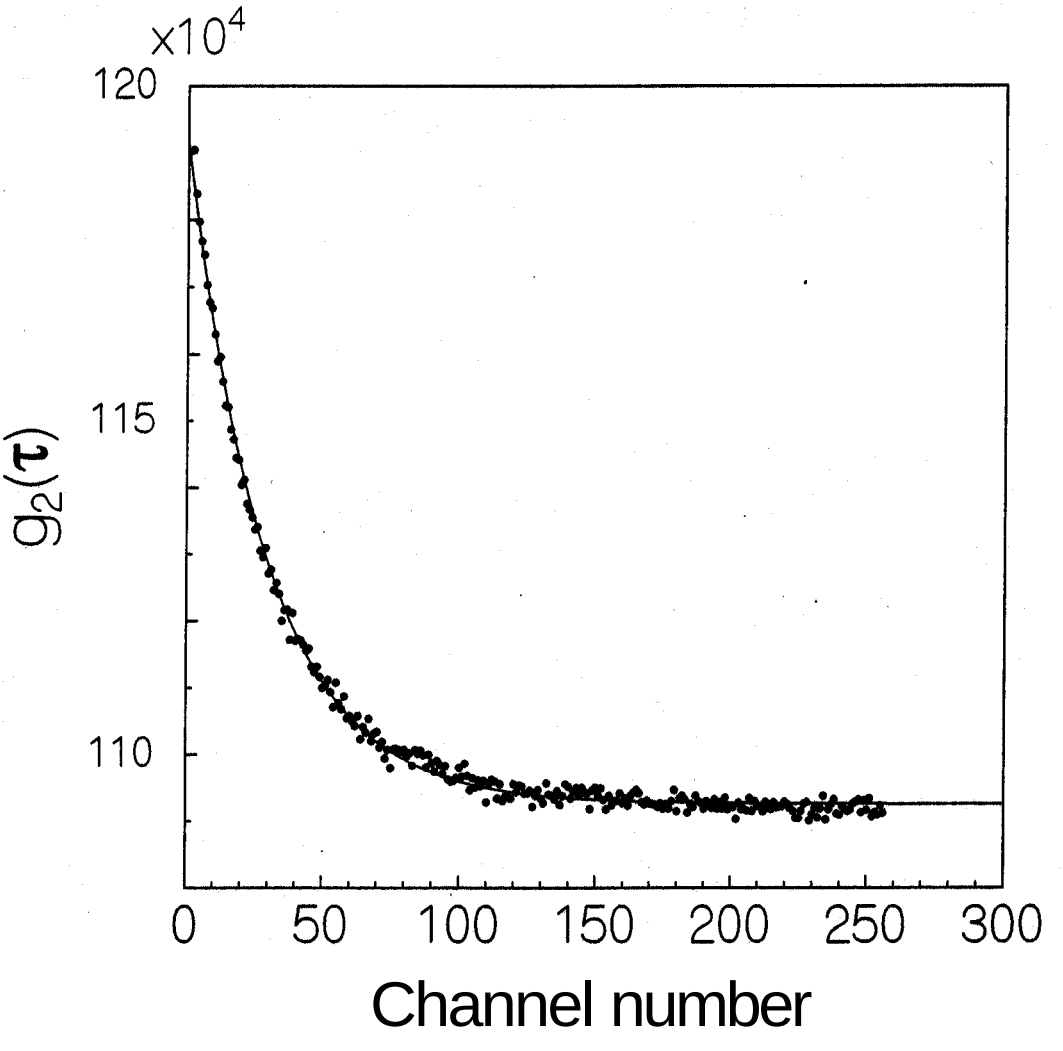

Figure 3.6: The figure shows a typical raw correlogram obtained from the correlator. The data was taken at a scattering angle of 95 degrees and with a delay time of 150μs. The total integration time was 300 seconds.

3.4 Data and error analysis

In this section we describe in detail the methods used by us for data analysis and error estimation.

3.4.1 Analysis of the intensity autocorrelation functions

The normalized intensity autocorrelation functions obtained in the experiments described in this chapter were fitted to a three parameter single exponential model of the type

$$g_2(\tau) = a_1 + a_2 e^{-(\tau)/a_3}$$

Here a_1 is called the base line parameter, a_2 is the strength of the decay and a_3 is the relaxation time. We are justified in using this one exponential decay rnodel since theoretical analysis shows that for the scattering geometry employed, one relaxation mode can be observed. We have used two programs to perform the non-linear curve fitting of our data. One of the programs worked out by us is based on the Levenberg-Marquadt minimization routine [6]. The other program was a part of a cornniercially available curve fitting and plotting package developed by CoHort Software. We found that parameters obtained froni both these programs were in good agreement with each other within rounding off errors. We have mostly used the CoHort package because it is more versatile. We checked the fitting routine for its robustness by feeding in different initial guess pararneters and running the program on the same data set. We found that the resulting parameters from the two programs did riot appreciably differ in their final values. As another check we used the pararneters obtained in one run as the guess paranieters for the next run on the same data set. In some cases we found that the output parameters don't converge to any particular value but oscillate between two values in consecutive runs. However, the values wcrc very close to each other differing only in the fourth decimal.

3.4.2 Analysis of the dispersion curve

A typical dispersion curve obtained in our experiments was fitted to a model of the type

$$\tau^{-1}(q) = b_1 q + b_2 q^2$$

Here, b_1 is a parameter and b_2 is the viscoelastic coefficient K_2/γ_1.

We know that the minimum value of $\tau^{-1}(q)$ occurs at $q = q_{opt} = 2q_o$.

$$\frac{\partial}{\partial q}\tau^{-1}(q)\Big|_{q=q_{opt}} = 0$$

$$b_1 + 2b_2 q_{opt} = 0$$

$$q_{opt} = -\left(\frac{b_1}{2b_2}\right) = 2q_o$$

Therefore, the pitch is given by,

$$P = -\frac{8\pi b_2}{b_1}$$

3.4.3 Error estimation

In the previous section we have described how we obtain b_1 and b_2 by fitting a model function to experimental data. Once the parameters have been obtained it is necessary to estimate the errors on them. The errors are a measure of the scatter of the data points. In this section we discuss the method we have used to estimate errors in the parameters. Given a data set we can fit it to a model having a certain number of parameters. For a given set of parameters we can define a measure of goodness of the fit, χ^2 as [7],

$$\chi^2 = \sum_i^N \left(\frac{y^i_{meas} - y(x_i)}{\sigma_i}\right) \tag{3.7}$$

Here y^i_{meas} is the experimentally measured value and $y(x_i)$ is the value predicted by the model corresponding to the ith value of the independent variable x. σ_i is the

uncertainty in the measurement of the ith valuc y^i_{meas}, and N is the total number of data points

In an experiment we measure a certain physical quantity. No experiment can measure the 'true' value of this quantity. There will always be a scatter in the results obtained from successive measurements on the same system. These values will follow a distribution function. The mean of this distribution function is the measured value (y_{meas}) and the standard deviation of the distribution will represent the uncertainty in measurement ***(a)***.It is useful to look upon χ^2 as,

$$\chi^2 = \sum_i^N \left(\frac{(observed\ \ deviation)_i}{(expected\ \ deviation)_i} \right)^2$$

If the model is good, then for a certain choice of parameters, the observed deviations will be comparable to the expected deviations. Each term in the summation above will be close to unity and we can write,

$$\chi^2 \approx N$$

We define the normalized χ^2 as,

$$\chi^2_N = \chi^2/N$$

Hence, for good fit,

$$\chi^2_N \approx 1$$

The value of χ^2_N is used to estimate the errors in the parameters obtained by curve fitting. The procedure used by us is outlined below.

- We first obtain the parameters for a particular model and call these as the mean values of the parameters.
- We determine the value of χ^2_N corresponding to the mean values of the parameters.
- Keeping other parameters fixed, we vary one of them in the vicinity of the mean valuc. At every varied valuc of the parameter we calculate the corresponding χ^2_N. We notice that either increasing or decreasing the valuc of the parameter will result in an increase in the valuc of χ^2_N. This parameter tuning process is shown in figure(**3.7).**

We determine by how much the parameter has to be changed to get a unit increase in χ^2_N. We call this value of the parameter as the varied value. The difference between this varied value and the mean value is an estimate of the error in the parameter.

A note on σ_i: In our experiments, the value of σ_i, the expected deviations in relaxation times from the true value is not known in advance. We obtain a rough estimate of the σ_i by a few repeated measurements at the same wavevector. The difference between the highest and the lowest relaxation times obtained is taken to be an estimate of σ_i. The average of the differences between the highest and the lowest relaxation times recorded at **a** few angles is used as a common σ_i for all wavevectors in the calculation of χ^2_N.

We have used the data and error analysis methods discussed in this section for analyzing the experimental data reported in this thesis.

3.5 Results and discussion

Dispersion curves for the twist fluctuation have been obtained in a regime where the wavelengths of the modes of director fluctuations are comparable to the pitch. By fitting the dispersion curves obtained at various temperatures to a generalized quadratic in q we can obtain the temperature dependence of the viscoelastic coefficient K_2/γ_1. Selective reflection experiments revealed that the pitch of the cholesteric mixture increases with temperature. Our results of the pitch obtained from selective reflection experiments are shown in figure(3.8).

The increase in pitch causes the angle θ to increase. At angles corresponding to 7.2°C below the cholesteric-isotropic transition, the Bragg reflection beams were not accessible to us in our experiment. This is due to the limitation of the goniometer arm getting obstructed by the laser stand at very high scattering angles. But the trend in the behavior of the viscoelastic coefficient K_2/γ_1 with temperature is clearly borne out by experimentally accessible wavevectors. The temperature variation of the twist viscoelastic coefficient is shown in figure (3.9). As one approaches the cholesteric-isotropic transition temperature, the twist viscoelastic coefficient shows a

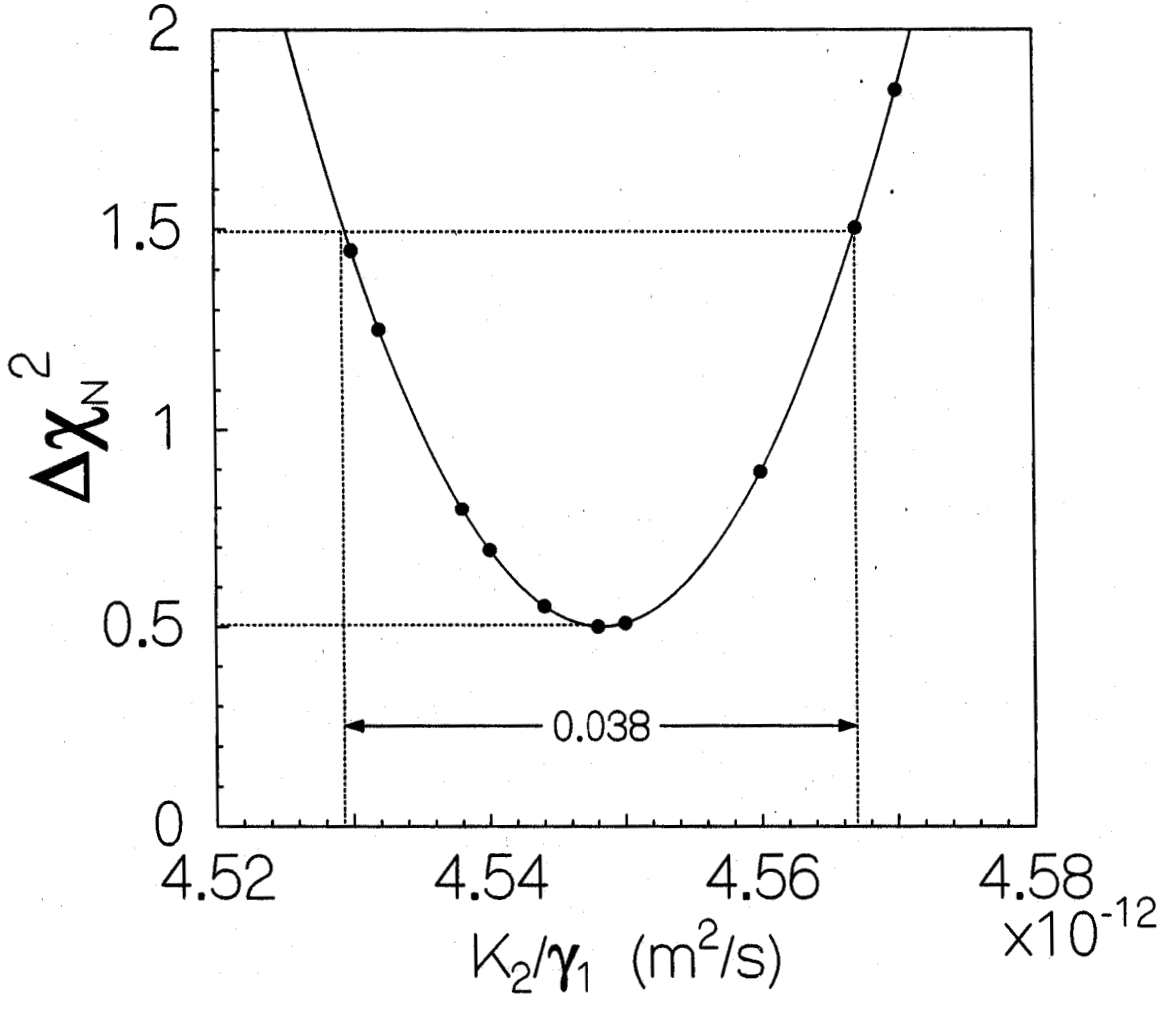

'Figure 3.7: The figure shows the change normalized χ^2_N as the value of the parameter K_2/γ_1 is varied about its mean value. The data was obtained at $40\pm0.05'$. In the example shown above, the value of K_2/γ_1 turns out to be $(4.548\pm0.019)\ x\ 10^{-12}m^2/s$.

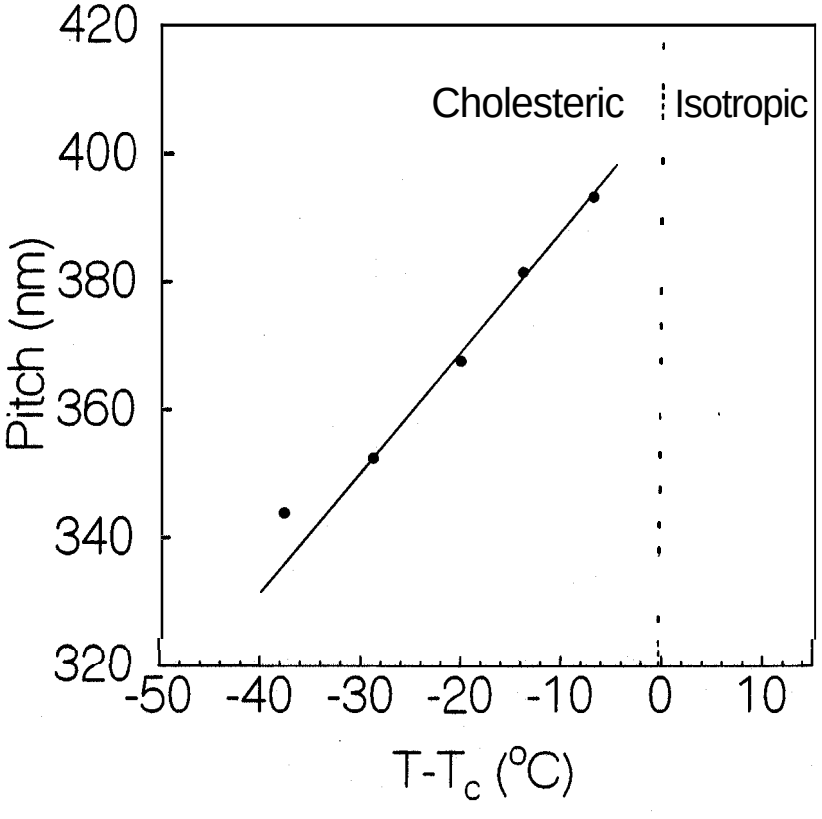

Figure **3.8:** Variation of pitch with temperature obtained by selective reflection experiments. T_c is cholesteric-isotropic transition temperature.

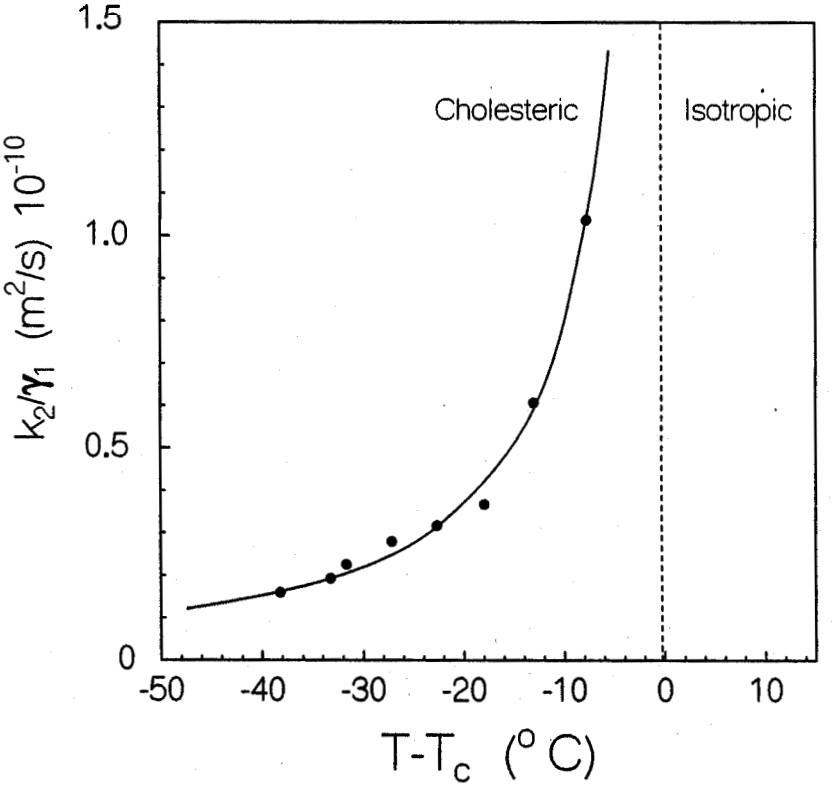

Figure 3.9: Variation of the twist viscoelastic coefficient k_2/γ_1 with temperature. T_c is cholesteric-isotropic transition temperature.

sharp increase. This is probably due to the weak first order or nearly second order nature of the transition at which $K_2 \to \infty$. A similar but less dramatic divergence of the viscoelastic coefficient with temperature has been observed in mixtures of side chain polymeric liquid crystals and low molar mass mesogens [1], [8].

In summary, we have studied the viscoelastic twist mode of director fluctuations in a thermotropic cholesteric liquid crystal. We have investigated twist dynamics of the cholesterics on a length scale comparable to the pitch. DuPre et. al., [3] have studied the twist mode in an entirely different wavevector regime in a lyotropic cholesteric liquid crystal. The pitch of the lyotropic cholesteric is approximately two orders of magnitude more than that of the thermotropic cholesteric studied by us. An important application of thermotropic liquid crystals is in displays. From our experiments we obtain temperature dependence of twist viscoelastic coefficient K_2/γ_1 which is an important parameter for selecting liquid crystals for use in displays.

Bibliography

[1] C. Fan, L. Kramer, and M. J. Stephen. *Phys. Rev. A, 2,* **2482 (1970).**

[2] R. W. Duke and D. B. Du Pre. *Mol. Cryst. Liq. Cryst.*, **43, 33 (1977).**

[3] R. W. Duke and D. B. Du Pre. *Phys. Rev. Letts., 67,* **67 (1974).**

[4] P. G. de Gennes and J. Prost. *The Physics of Liquid Crystals* , 2nd ed., Clarendon press, Oxford **(1993).**

[5] S. Chandrasekhar. *Liquid Crystals* , 2nd ed., Cambridge University press, Cambridge **(1992).**

[6] S. **A.** Teukolsky, W. H. Press W. T. Vetterling, and B. P. Flannery. *Numerical Recipes in C:The Art of Scientific Computing.* Cambridge University Press, Cambridge **(1988).**

[7] P. **R.** Bevington. *Data Reduction and Error Analysis for the Physical Sciences.* McGraw-Hill, London, **(1969).**

[8] M. S. Sefton, **A.** R. Bowdler, and H. J. Coles. *Mol. Cryst. Liq. Cryst.*, **129,** 1 **(1 985).**

[9] Pei-Yuan Liu, Ning Yao, and Alex M. Jamieson. *Macromolecules,* **32, 6587(1999).**